Asociación Argentina
de Mecánica Computacional

Mecánica Computacional Vol XXIX, págs. 2407-2416 (artículo completo)
Eduardo Dvorkin, Marcela Goldschmit, Mario Storti (Eds.)
Buenos Aires, Argentina, 15-18 Noviembre 2010

A MULTISCALE FINITE ELEMENT METHOD APPLIED TO A NEUROSCIENCE PROBLEM

Alexandre L. Madureira and Daniele Q.M. Madureira

Departamento de Matemática Aplicada , Laboratório Nacional de Computação Científica , Av. Getúlio Vargas 333 , 25651-070 , Petrópolis - RJ, Brazil

Keywords: multiscale, neuroscience, finite elements, cable equation.

Abstract. Several interesting problems in neuroscience are of multiscale type, i.e. possesses different temporal and spatial scales that cannot be disregarded. Such characteristics impose severe burden to numerical simulations since the need to resolve small scale features push the computational costs to unreasonable levels. Classical numerical methods that do not resolve the small scales suffer from spurious oscillations and lack of precision. This paper presents a finite element method of multiscale type that is easy to parallelize and that ameliorates these maladies. We show the validity of our scheme under different physiological regimes.

Copyright © 2010 Asociación Argentina de Mecánica Computacional http://www.amcaonline.org.ar

1 INTRODUCTION

Among the fields of research that computer models can hope to deliver significant contributions, neuroscience is one of the most demanding and beautiful. Among the main aspects that makes neuroscience so challenging from the modeling and computational point of view are the multiple temporal and spatial scales present in most neurological events. Some instances of what is steadly being considered in present research are attempts to increase the size of networks of spiking neurons, as well as incorporation of spatial and heterogeneous aspects of the neuron physiology. Although the ever increasing capabilities of computers facilitate such endeavors, a big chunk of the advances are certainly due to better modeling and computational techniques.

We focus here on the task of deriving an efficient numerical method for problems of multiscale type. The problem we consider involves modeling dendrites with an uneven distribution of synapses. A recent important paper (Meunier and Lamotte d'Incamps, 2008) considered various instances of heterogeneous dendrites modeled by variants of cable equations, and inquired when the process of *mathematical homogenization* was valid. The trouble is, the homogenization process is valid only *as the number of heterogeneities approach infinity*. That is not the whole story, since the heterogeneity must have some sort of "pattern", being periodic or random for instance. Such assumptions are often questionable.

Motivated by such concerns, we investigate the same cable equation problem considered in (Meunier and Lamotte d'Incamps, 2008), this time from a numerical point of view. Let the voltage $\hat{V}$ be the solution of the cable equation

$$\begin{gathered} c_m \frac{\partial V}{\partial t} - \frac{\sigma^{\mathrm{l}} d}{4} \frac{\partial^2 \hat{V}}{\partial \hat{x}^2} + \sigma^{\mathrm{m}} \hat{V} + \hat{\sigma}^{\mathrm{in}}(\hat{V} - V^{\mathrm{in}}) + \hat{\sigma}^{\mathrm{ex}}(\hat{V} - V^{\mathrm{ex}}) = 0 \quad \text{in } (0, L) \times (0, +\infty). \\ \hat{V}(0, t) = \hat{V}(L, t) = 0 \quad \text{for } t \in (0, +\infty), \\ \hat{V}(x, 0) = V_0(x) \quad \text{for } x \in (0, L). \end{gathered} \tag{1}$$

Above, V_0 is the initial condition, d denotes the dendrite diameter in centimeters (cm), c_m is the specific membrane capacitance in Farad per square centimer (F/cm^2), σ^{l} denotes the longitudinal dendrite specific conductance in siemens per centimeter (S/cm), σ^{m} denotes the membrane specific conductance in siemens per square centimeter (S/cm^2), and $\hat{\sigma}^{\mathrm{ex}}$ and $\hat{\sigma}^{\mathrm{in}}$ are the excitatory and inhibitory synapse specific conductance, also in siemens per square centimeter (S/cm^2). We assume that the specific conductances σ^{l} and σ^{m} are constant. The potentials $\hat{V}$, V^{ex} and V^{in} are in millivolt (mV), and both reversal potentials V^{ex} and V^{in} are constant. Finally, L is the dendrite length in centimeter (cm). The synapses are modeled by

$$\hat{\sigma}^{\mathrm{in}} = \sum_{l=1}^{N^i} g_l^i \delta_{\hat{x}_l^i}, \qquad \hat{\sigma}^{\mathrm{ex}} = \sum_{l=1}^{N^e} g_l^e \delta_{\hat{x}_l^e},$$

where $\delta_{\hat{x}_l^i}$ are Dirac deltas (or delta "functions") located at the synapses sites $\hat{x}_l^i$ with strenghts g_l^i, for $l = 1, \ldots, N^i$. Similar notation holds for the excitatory synapses, i.e., the deltas $\delta_{x_l^e}$ are located the synapse sites $\hat{x}_l^e$ with strenghts g_l^e, for $l = 1, \ldots, N^e$. The definition of a Dirac delta $\delta_{\hat{x}^*}$ located at a point $\hat{x}^* \in (0, L)$ is that

$$\int_0^L \delta_{\hat{x}^*} g(\hat{x})\, d\hat{x} = g(\hat{x}^*), \tag{2}$$

for any continuous function g.

Copyright © 2010 Asociación Argentina de Mecánica Computacional http://www.amcaonline.org.ar

For equations like (1), several different numerically demanding instances might show up, as big differences in the strenghts of the synapses, large number of synapses at uneven locations, and even a high ratio between the diameter of the dendrite and its lenght. Under these circunstances, the computational costs involved in solving such problems can be unacceptable if a raw numerical method is to be considered, in particular when considering a large tree of dendrites where each branch is modeled by (1). The computational costs grow since *any* method employed has to account for the microscale aspects of the dendrite physiology.

In the computational neuroscience literature, discretization of spatial features of partial differential equations traditionally employs compartmental models and difference schemes. On the other hand, finite elements are seldom employed. This is unfortunate since methods based on finite elements are flexible, simple to implement, computationally efficient, and easier to analyse. For "nice" problems, when the solution has a smooth behaviour and there is no numerical complications, finite elements and finite differences yield comparable resuls. However, because of its attributes, when standard schemes do not work well, modern variants of finite elements come as an viable option of discretization.

One variant is the multiscale finite element method (Hou, 2003), which we explore here. The idea behind multiscale methods to solve heterogeneous systems is that one has to first solve some *local problems* and extract some *microscale information*. Such information is then *upscaled* into a *homogenized* macroscale problem. Microscale problems depend on refined information of the model, but has to be solved in *small domains*, and parallelization is trivial. Due to this local feature, they are not so expensive to solve. In contrast, the homogenized macroscale problem is global and has to be solved in the whole domain. But the microscale data show up averaged, i.e., *homogenized*, and the cost of solving the homogenized macroscale problem is independent of the microscales. As a bonus, for one-dimensional domains, the multiscale finite element method yields a *nodally exact solution*, i.e., the numerical solution matches the exact solution at each nodal point.

As an example, consider a thin dendrite with synapses distributed along its extension. The voltage will jump at the sysnapses locations, and since traditional methods must use a huge number of grid points to capture such small scale behavior, they quickly become impractical. On the other hand, the multiscale finite element method global problem uses a fixed number of grid points, independent of the number of synapses and the thickness of the dendrite. Between each two consectutive grid points, a subgrid is created and smaller local problems are solved, possibly in parallel, and microscale information are uploaded to the global problem that is solved afterwards. We emphasize that the costs associated with solving the final global problem is independent of all physiological parameters.

We now describe briefly the contents of the present paper. In the next section, we present the basics of the multiscale finite element method applied to (1). Next, in Section 3 we analyse the behaviour of the model under different limit situations, and display some numerical results. We present our conclusions in Section 4.

Copyright © 2010 Asociación Argentina de Mecánica Computacional http://www.amcaonline.org.ar

2 THE MULTISCALE FINITE ELEMENT METHOD (MSFEM)

To facilitate the dissection of the main properties of the problem under consideration, it is convenient first to define new coordinates $x = \hat{x}/L$, and rewrite (1) as

$$\begin{gathered} \tau_m \frac{\partial V}{\partial t} - \epsilon \frac{\partial^2 V}{\partial x^2} + V + GV = f \quad \text{in } (0,1) \times (0,+\infty), \\ V(0,t) = V(1,t) = 0 \quad \text{for } t \in (0,+\infty), \\ \hat{V}(x,0) = V_0(x) \quad \text{for } x \in (0,L). \end{gathered} \tag{3}$$

where $V(x,t) = \hat{V}(Lx,t)$,

$$\tau_m = \frac{c_m}{\sigma^{\mathrm{m}}}, \qquad \epsilon = \frac{\sigma^{\mathrm{l}} d}{4L^2 \sigma^{\mathrm{m}}}, \qquad G = \frac{\sigma^{\mathrm{in}} + \sigma^{\mathrm{ex}}}{\sigma^{\mathrm{m}}}, \qquad f = \frac{\sigma^{\mathrm{in}} V^{\mathrm{in}} + \sigma^{\mathrm{ex}} V^{\mathrm{ex}}}{\sigma^{\mathrm{m}}}.$$

We also have

$$\sigma^{\mathrm{in}} = \sum_{l=1}^{N^i} g_l^i \delta_{x_l^i}, \qquad \sigma^{\mathrm{ex}} = \sum_{l=1}^{N^e} g_l^e \delta_{x_l^e}, \tag{4}$$

where the Dirac deltas are now located at the sites $x_l^i = \hat{x}_l^i/L$, and $x_l^e = \hat{x}_l^e/L$.

The *variational formulation*, is given by

$$\int_0^1 \tau_m \frac{\partial V}{\partial t} w \, dx + \int_0^1 \left(\epsilon \frac{\partial V}{\partial x} \frac{\partial w}{\partial x} + Vw + GVw \right) dx = \int_0^1 fw \, dx. \tag{5}$$

for all $w \in H_0^1(0,1)$. Using (4), and the definition of Dirac deltas (2), it follows that

$$\int_0^1 GVw \, dx = \sum_{l=1}^{N^i} \frac{g_l^i V(x_l^i) w(x_l^i)}{\sigma^{\mathrm{m}}} + \sum_{l=1}^{N^e} \frac{g_l^e V(x_l^e) w(x_l^e)}{\sigma^{\mathrm{m}}},$$

$$\int_0^1 fw \, dx V^{\mathrm{in}} \sum_{l=1}^{N^i} \frac{g_l^i w(x_l^i)}{\sigma^{\mathrm{m}}} + V^{\mathrm{ex}} \sum_{l=1}^{N^e} \frac{g_l^e w(x_l^e)}{\sigma^{\mathrm{m}}}.$$

2.1 The definition of the multiscale method

We first decompose the domain $(0,1)$ in the *elements* (x_0, x_1), $(x_1, x_2), \ldots, (x_{N-1}, x_N)$, (x_N, x_{N+1}), definined by the nodes

$$0 = x_0 < x_1 < x_2 < x_3 < \cdots < x_N < x_{N+1} = 1. \tag{6}$$

We approximate V by the *multiscale function* V_h^{ms} defined by

$$V_h^{\mathrm{ms}}(x,t) = \sum_{k=1}^{N} V_k^{\mathrm{ms}}(t) \lambda_k(x). \tag{7}$$

The unknowns $V_1^{\mathrm{ms}}(t), \ldots, V_N^{\mathrm{ms}}(t)$ depend on t only. The new basis functions $\{\lambda_1, \ldots, \lambda_N\}$ are continuous, but instead of being linear within each element, they satisfy the local, elementwise problems

$$\begin{gathered} \lambda_k(x) = 0 \quad \text{if } x \notin (x_{k-1}, x_{k+1}), \\ -\epsilon \frac{\partial^2 \lambda_k}{\partial x^2} + \lambda_k + G\lambda_k = 0 \quad \text{in } (x_{k-1}, x_k) \text{ and } (x_k, x_{k+1}), \\ \lambda_k(x_k) = 1, \end{gathered} \tag{8}$$

Copyright © 2010 Asociación Argentina de Mecánica Computacional http://www.amcaonline.org.ar

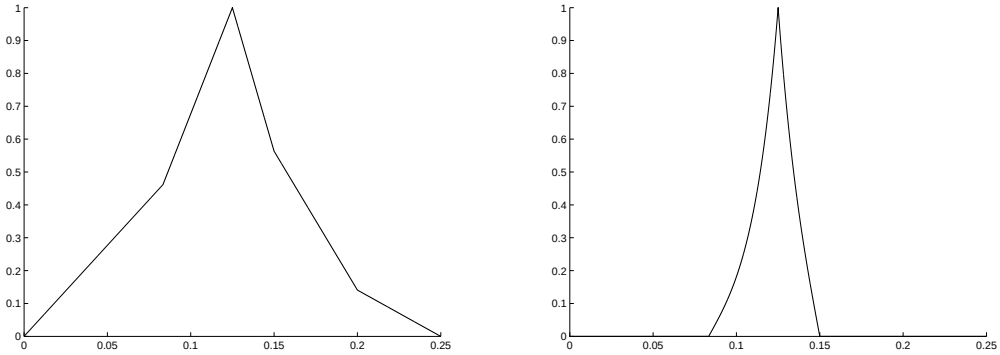

Figure 1: Typical multiscale basis functions

for $k \in \{1, \ldots, N\}$.

In a few particular cases it is possible to compute λ_k explicitely, but in general it is necessary to approximate it numerically. In Figure 1 we depict typical basis functions. The domain is assembled joining two consecutive elements, and it contains two inhibitory sysnapses at 0.08 and 0.15, and a excitatory syspse at 0.2. The function in the left was obtained for large ϵ, and the one in the right for small ϵ.

It is worth pointing out that these basis functions adapt and capture the local physiological heterogeneities effects of the dendrites. If there are synapses, the functions have jumps in their derivatives, as the exact solution of the original problem does. If ϵ is small, the functions have a exponential profile, just like the solution of the original problem. That is how the upscaling process occur. Note that in classical elements, the functions would be piecewise linear, regardless of the parameters.

As long as the multiscale basis functions λ_k are computed, the unknowns $V_1^{\text{ms}}, \ldots, V_N^{\text{ms}}$ are defined by:

$$\sum_{k=1}^{N} \tau_m \frac{dV_k^{\text{ms}}}{dt} \int_0^1 \lambda_k(x)\lambda_j(x)\,dx + V_k^{\text{ms}} \int_0^1 \left[\epsilon \frac{\partial \lambda_k(x)}{\partial x} \frac{\partial \lambda_j(x)}{\partial x} + \lambda_k(x)\lambda_j(x) + G\lambda_k(x)\lambda_j(x) \right] dx = \int_0^1 f\lambda_j(x)\,dx \quad \text{for } j = 1, \ldots, N. \quad (9)$$

With such choice of basis functions, it is now possible to have an accurate method with the size of the system (9) *independent of* ϵ *and the number of synapses*. The task of incorporating the microstructure, where the synapses play a direct role and rise the costs, is concentrated in the computation of the basis functions. That is the subject of the next subsection.

As we already remarked, a striking property of multiscale methods is that, for steady state one-dimensional domains, the numerical solution yields the exact solution at *every node*. Such property follows from the very definition of the method, i.e. from (8) and (9).

3 DIFFERENT REGIMES AND THEIR SOLUTIONS

As pointed out previously, varying the different parameters in (1) lead to different various neurological regimes in the solution. In many instances this causes spurious oscillatory behaviour in numerical computations. To understand the different behaviour that show up, it is useful to perform an analysis using (3). We consider here only the non-transient problem.

Copyright © 2010 Asociación Argentina de Mecánica Computacional http://www.amcaonline.org.ar

As an example, consider the case when ϵ is much smaller than one ($\epsilon \ll 1$). This happens for instance when the dendrite is too thin or too long ($d \ll L^2$), when the longitudinal conductance is too big ($\sigma^{\mathrm{l}} \gg \sigma^{\mathrm{m}}$), or when a combination of the above features occur. In such cases numerical difficulties appear, as we shall see. Another different situation is when there is a huge number of synapses, or when the membrane conductance is either too large or too low. In what follows, we present separate formal studies of these *asymptotic limits* and show how the classical and mustiscale finite elements perform. To exalt the effects of each separate situation, we isolate each one of them using paramenters that are not necessarily biologically plausible.

3.1 Long or thin dendrites, or small longitudinal conductance

One situation where numerical difficulties occur is when the parameter ϵ is too small. In terms of physiology of the dendrites there are many instances when this can happen, as described above. However, regardless of the origins, the numerical outcomes are the same.

To find out how the solution V depends on the parameter ϵ, we use the method of matching asymptotics, postulating that

$$V(x) \sim V_0(x) + \epsilon V_1(x) + \epsilon^2 V_2(x) + \dots, \tag{10}$$

where the functions V_j are to be determined. Formally replacing (10) in (3), we gather that

$$V_0 + GV_0 + \epsilon\left(-\frac{\partial^2 V_0}{\partial x^2} + V_1 + GV_1\right) + \epsilon^2\left(-\frac{\partial^2 V_1}{\partial x^2} + V_2 + GV_2\right) + \dots = f \quad \text{in } (0,1).$$

Collecting the $\epsilon = 0$ limit terms, it follows that $V_0 + GV_0 = f$, i.e.,

$$\sigma^{\mathrm{m}} V_0 + \left(\sum_{l=1}^{N^i} g_l^i \delta_{x_l^i} + \sum_{l=1}^{N^e} g_l^e \delta_{x_l^e}\right) V_0 = \sum_{l=1}^{N^i} g_l^i \delta_{x_l^i} V^{\mathrm{in}} + \sum_{l=1}^{N^e} g_l^e \delta_{x_l^e} V^{\mathrm{ex}}$$

After a multiplication by an arbitrary and smooth function ϕ, and an integration, the above equation becomes

$$\int_0^1 \sigma^{\mathrm{m}} V_0 \phi \, dx + \sum_{l=1}^{N^i} g_l^i V_0(x_l^i)\phi(x_l^i) + \sum_{l=1}^{N^e} g_l^e V_0(x_l^e)\phi(x_l^e) = V^{\mathrm{in}} \sum_{l=1}^{N^i} g_l^i \phi(x_l^i) + V^{\mathrm{ex}} \sum_{l=1}^{N^e} g_l^e \phi(x_l^e).$$

By considering special functions ϕ (actually, a sequence of them), it is possible to prove that

$$V_0(x) = \begin{cases} 0 & \text{if } x \notin \{x_1^i, \dots, x_{N^i}^i, x_1^e, \dots, x_{N^e}^e\}, \\ V^{\mathrm{in}} & \text{if } x \in \{x_1^i, \dots, x_{N^i}^i\}, \\ V^{\mathrm{ex}} & \text{if } x \in \{x_1^e, \dots, x_{N^e}^e\}. \end{cases}$$

Thus, as $\epsilon \to 0$, the exact solution V approaches the discontinuous function V_0. Since V itself is continuous, there is an onset of internal layers at the points of discontinuity. These layers cause severe numerical trouble.

Such behaviour of the exact solution does not come as a surprise. Indeed the neurological meaning of "ϵ small" is that there is relatively little diffusion of ions, as occur when the dendrite is thin, or the longitudinal conductance is small. In such instance, the electric "jumps" that take place at the synapses concentrates in a narrow neighborhood of the synaptic loci.

Copyright © 2010 Asociación Argentina de Mecánica Computacional http://www.amcaonline.org.ar

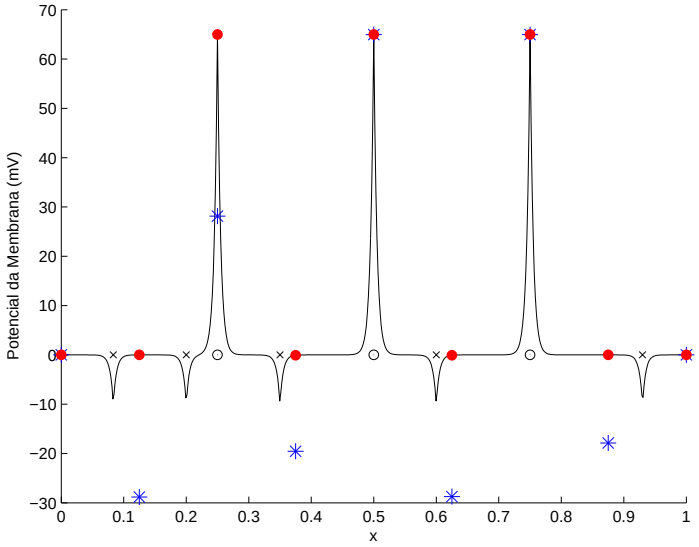

Figure 2: Exact Solution

As a numerical test, depicted in Figure 2, we pick an example where five inhibitory (location marked with an $\times$) and three excitatory (location marked with an $\odot$) synapses are disposed along the dendrite, $V^{\text{in}} = -10$, $V^{\text{ex}} = 65$, and $\epsilon = 2.5 \times 10^{-5}$. In this example, and all that follow, an "exact solution" (displayed in solid black line) is numerically computed by "overkill", using a numerical method with a sufficiently refined mesh. We solve the same problem using classical (computed nodal values marked by asterisks) and multiscale finite element methods (computed nodal values marked by red dots), with nine nodal points in both cases.

We first comment on the exact solution. Observe that it is close to zero except in a small neighborhood of the synapses. Over the synapses the value of the exact solution is close to either $V^{\text{in}} = -10$ or $V^{\text{ex}} = 65$. This confirms our theoretical prediction that, whenever ϵ is small, V should be close to V_0. Regarding the numerical aspects, the classical method yields a solution that is essentially wrong, where the multiscale solution matches the exact solution at every node, as predicted by the theory. Sure enough, if sufficient points are used in the classical scheme, we would eventually obtain a reasonable approximation. For instance, for the present example, 129 points are necessary to bring the relative errors within a range of 10% at every node.

3.2 Large number of synapses

Suppose that $N^i = N^e$, and that $\alpha = 1/(2N^i)$. Assume further that the synapses are disposed periodically, i.e., the Dirac deltas are located at the sites $x_l^i = (2l-1)\alpha$ and $x_l^e = 2l\alpha$. In the present case, the interest is when the synapses are narrowly packed, i.e. $\alpha \ll 1$, and this situation is tricky to analyse.

The idea is to rewrite the solution of (3) as the minimizer of the energy

$$J(V) + \alpha^{-1} I_\alpha(V), \tag{11}$$

Copyright © 2010 Asociación Argentina de Mecánica Computacional http://www.amcaonline.org.ar

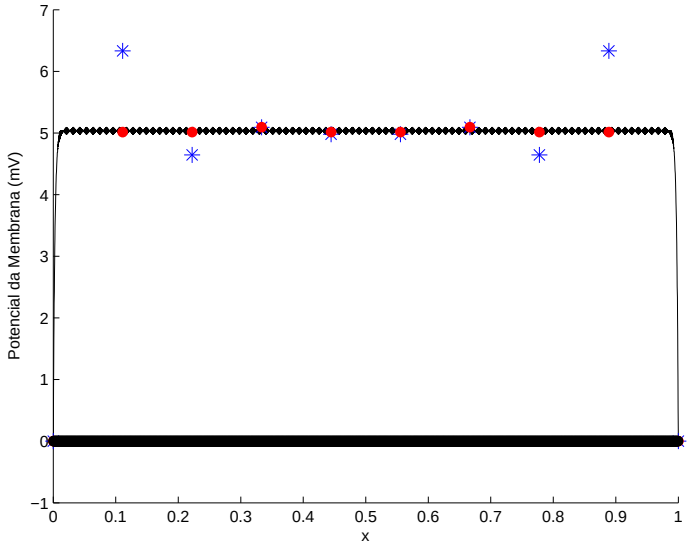

Figure 3: Exact Solution

where

$$J(V) = \frac{1}{2}\int_0^1 \epsilon\sigma^{\mathrm{m}}\left(\frac{\partial V}{\partial x}\right)^2 + \sigma^{\mathrm{m}}V^2\,dx,$$

$$I_\alpha(V) = \frac{\alpha}{2}\sum_{l=1}^{N^i} g_l^i V^2(x_l^i) + \frac{\alpha}{2}\sum_{l=1}^{N^e} g_l^e V^2(x_l^e) - \alpha V^{\mathrm{in}}\sum_{l=1}^{N^i} g_l^i V(x_l^i) - \alpha V^{\mathrm{ex}}\sum_{l=1}^{N^e} g_l^e V(x_l^e).$$

Under reasonable conditions on g_l^i and g_l^e, as $\alpha \to 0$ the term I_α concentrates most of the total energy. Thus $\lim_{\alpha\to 0} V = V_0$ in a reasonable mathematical sense, where V_0 minimizes $\lim_{\alpha\to 0} I_\alpha$, and it turns out that

$$V_0 = \frac{V^{\mathrm{in}} g_l^i + V^{\mathrm{ex}} g_l^e}{g_l^i + g_l^e}$$

does the job.

As a numerical test, we consider the case of 2000 inhibitory and excitatory synapses, $g_l^i = 4\times 10^{-2}$, $g_l^e = 10^{-2}$, $V^{\mathrm{in}} = -10$, and $V^{\mathrm{ex}} = 65$. In this case, $V_0 = 5$, and that is exactly the number around which the solution oscillates. Numerically we consider ten nodal points for both methods. Note that the classical method (blue asterisks) oscillates close to the boundaries, but delivers a reasonable approximation in the interior of the domain. The multiscale method (red dots) is nodally exact, as it should be.

3.3 Large or low membrane conductance

The situation gets much simpler if

$$\sigma^{\mathrm{m}} \gg \max\left\{\frac{\sigma^{\mathrm{l}} d}{4L^2}, g_1^i, \ldots, g_{N^i}^i, g_1^e, \ldots, g_{N^e}^e, \right\}$$

or

$$\sigma^{\mathrm{m}} \ll \min\left\{\frac{\sigma^{\mathrm{l}} d}{4L^2}, g_1^i, \ldots, g_{N^i}^i, g_1^e, \ldots, g_{N^e}^e, \right\}.$$

Copyright © 2010 Asociación Argentina de Mecánica Computacional http://www.amcaonline.org.ar

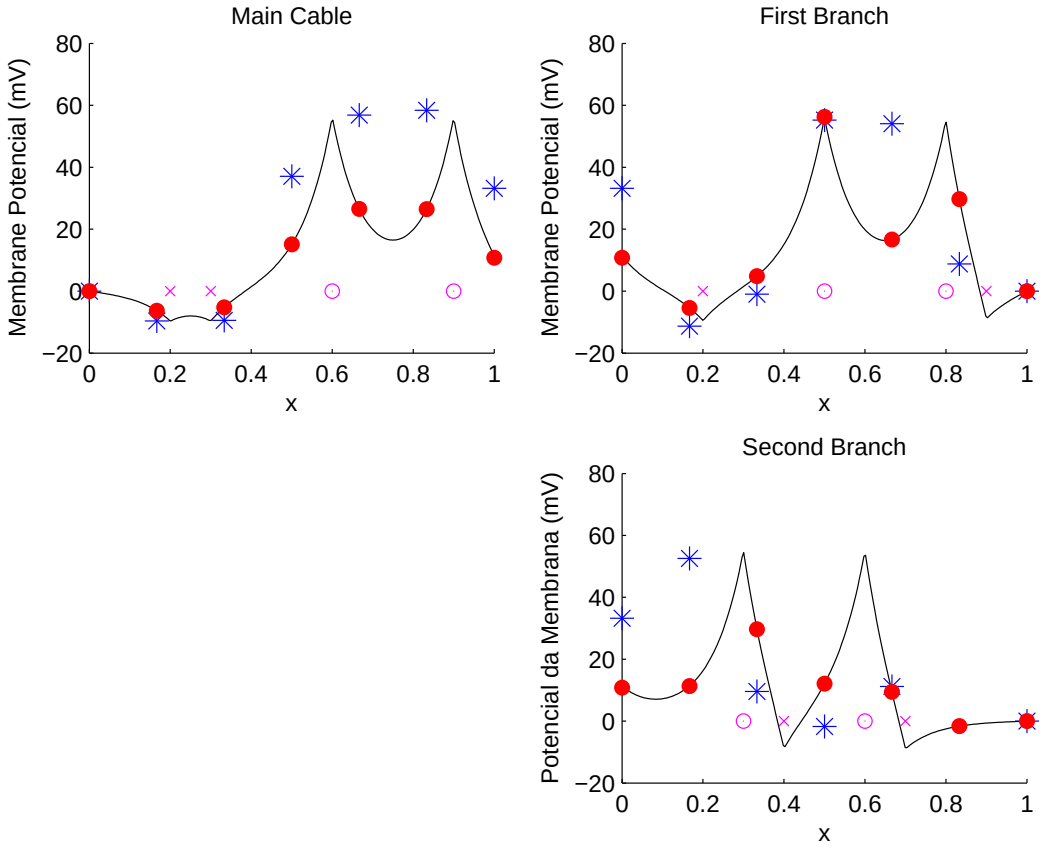

Figure 4: Branched solution.

The former case occur when the membrane is too "diffusive", allowing the transmembrane free flow of ions. Thus, the $V = 0$ limit comes as no surprise. In the latter situation, as $\sigma^{\mathrm{m}} \to 0$, V satisfies

$$\begin{aligned} -\frac{\sigma^{\mathrm{l}} d}{4L^2}\frac{\partial^2 V}{\partial x^2} + (\sigma^{\mathrm{in}} + \sigma^{\mathrm{ex}})V = \sigma^{\mathrm{in}} V^{\mathrm{in}} + \sigma^{\mathrm{ex}} V^{\mathrm{ex}} \quad \text{in } (0,1), \\ V(0) = V(1) = 0, \end{aligned} \tag{12}$$

reflecting the fact that the cross membrane flow of ions occur only through the synapses.

3.4 branched dendrite

We test here two situations not considered before. We first consider the steady state version of (1) in a Y-shapped domain. At the branching point, we impose continuity of voltage and current. The model is no longer provably nodally exact, but it still yields an excellent approximation for the exact solution.

In the figure 4 below, $V^{\mathrm{in}} = -10$, $V^{\mathrm{ex}} = 65$, $L = 0.2$, $d = 0.01$, $\sigma^{\mathrm{l}} = 10^{-3}$ and $\sigma^{\mathrm{m}} = 10^{-2}$ for all the branches, and there two excitatory and two inhibitory syspses in each of the banches. We used seven nodal points for both the classical and multiscale method. There is one nodal value for the classical method missing: the classical scheme yielded a value below -20.

It is notable that few points give excellent accuracy, and that allows for great efficiency when several branches are coupled.

Copyright © 2010 Asociación Argentina de Mecánica Computacional http://www.amcaonline.org.ar

4 CONCLUSIONS

Several models in neuroscience are of multiscale type, and classical numerical methods do not deal with them in a natural way, but rather requires brute force, also known as refined discretization, to capture physiological details. We present here a viable numerical alternative.

The problem we consider here depend in a nontrivial way in several parameters. In our case by case analysis, we show how the solutions depend on them. In practice, such extreme and isolated situations are unlikely. Biologically plausible examples exhibit actually a *combination* of these effects, in an attenuated fashion, but when using classical numerical approximations that might lead a disastrous net effect.

Homogenization techniques can help in some regimes, but they reliable only under very specific circunstances. On the other hand, our method is always robust, accurate, it is actually *nodally exact*, and parallelizable.

REFERENCES

Hou T.Y. Numerical approximations to multiscale solutions in partial differential equations. In *Frontiers in numerical analysis (Durham, 2002)*, Universitext, pages 241–301. Springer, Berlin, 2003.

Meunier C. and Lamotte d'Incamps B. Extending cable theory to heterogeneous dendrites. *Neural Comput.*, 20(7):1732–1775, 2008. ISSN 0899-7667. doi:10.1162/neco.2008.12-06-425.

Copyright © 2010 Asociación Argentina de Mecánica Computacional http://www.amcaonline.org.ar